Aalborg Universitet

On the hydrothermal depolymerisation of kraft lignin using glycerol as a capping agent

Ahlbom, Anders; Maschietti, Marco; Nielsen, Rudi; Hasani, Merima; Theliander, Hans

[Link to publication from Aalborg University](#)

Original Article

Anders Ahlbom, Marco Maschietti, Rudi Nielsen, Merima Hasani* and Hans Theliander

On the hydrothermal depolymerisation of kraft lignin using glycerol as a capping agent

Abstract: Depolymerisation of kraft lignin under hydrothermal conditions was investigated at short residence times (1–12 min) with glycerol being used as a capping agent. The weight average molecular weight (M_w) of the products decreased within the first minute of residence time, with the inter-unit ether linkages breaking accordingly. Furthermore, the M_w of the product fractions decreased at increasing residence times, while the char yield increased. Short residence times thus appear to be beneficial for mitigating the formation of char. Also, addition of NaOH reduced the yield of char. Although the addition of glycerol caused a decrease in the M_w of the products, it seemed to increase the yield of char and therefore might not be a suitable capping agent for kraft lignin depolymerisation.

Keywords: depolymerisation; glycerol; HTL; hydrothermal liquefaction; kraft lignin.

1 Introduction

Lignin, with its high content of aromatic rings, is perhaps the most important future source of renewable aromatic components for chemicals, materials and fuel additives. In order to extract these aromatic sub-units, however, its structure needs to be broken down in a controlled way: the lignin must be depolymerised (Dunn and Hobson 2016). Whilst several methods for doing this have been investigated, including pyrolysis, hydrotreatment, oxidation and catalytic methods, interest in hydrothermal methods has also been shown, and especially so due to the tunability of the yield of products at different processing temperatures. Low temperatures of around 200 °C result in carbonisation whereas intermediate temperatures of 300–350 °C favour liquefaction, and higher temperatures, especially around 600–700 °C, favour gasification of the feedstock (Kruse and Dahmen 2015).

Hydrothermal processes employ water at high pressure and temperature. At these conditions, a vast number of reactions will occur: various bonds in the lignin structure will be broken, but there will also be a certain amount of repolymerisation. One great benefit is that this process uses water, so there is no need to pre-dry the raw material (Castello et al. 2018). By working close to, but below, the critical point of water (374 °C and 221 bar) the ionic product is high, which leads to a higher concentration of OH^- and H_3O^+ as the water molecules dissociate (Kruse and Dahmen 2015). This favours ionic reactions, such as hydrolysis. Furthermore, near the critical point, the weaker hydrogen bonding between water molecules and the lower dielectric constant mean that water is better at dissolving non-polar molecules (Carr et al. 2011; Lappalainen et al. 2020; Peterson et al. 2008).

A problem associated with the depolymerisation of lignin is the production of reactive fragments: these may react with each other and cause the products to repolymerise. Such repolymerisation may lead to the production of char, which lowers the yield of useful products and hampers the processing because it may deposit on equipment and block flow (Belkheiri et al. 2014; Rößiger et al. 2018). The formation of char can be mitigated by the addition of capping agents, which are chemicals that react with the reactive fragments and thereby hinder them from charring. Furthermore, reaction parameters such as temperature and residence time influence the amount of char produced in the process (Otromke et al. 2019).

Capping agents that have been investigated previously in the hydrothermal processing of lignin include boric acid (Roberts et al. 2011), phenol (Arturi et al. 2017; Belkheiri et al. 2018; Nguyen et al. 2014; Saisu et al. 2003) and aliphatic alcohols such as methanol (Belkheiri et al. 2014; Cheng et al. 2016), ethanol (Cheng et al. 2012; Lee et al. 2016) and butanol (Yoshikawa et al. 2013).

*Corresponding author: Merima Hasani**, Department of Chemistry and Chemical Engineering, Chalmers University of Technology, SE-412 96 Gothenburg, Sweden, E-mail: merima.hasani@chalmers.se
Anders Ahlbom and Hans Theliander, Department of Chemistry and Chemical Engineering, Chalmers University of Technology, SE-412 96 Gothenburg, Sweden, E-mail: anders.ahlbom@chalmers.se (A. Ahlbom), hanst@chalmers.se (H. Theliander). https://orcid.org/0000-0002-5055-041X (A. Ahlbom)
Marco Maschietti and Rudi Nielsen, Department of Chemistry and Bioscience, Aalborg University, Niels Bohrs Vej 8, 6700 Esbjerg, Denmark, E-mail: marco@bio.aau.dk (M. Maschietti), rudi@bio.aau.dk (R. Nielsen)

In a previous study carried out by this group (Ahlbom et al. 2022), based on the use of isopropanol as a capping agent at short residence times, it was shown that the reactions proceed rapidly to cleave inter-unit ether linkages in the lignin within 1 min while the char yield increased at longer residence times. Furthermore, adding isopropanol to the reaction system caused a decrease not only in the char yield but also in the weight average molecular weight (M_w) of the products (Ahlbom et al. 2021). Investigating the use of other types of alcohols as capping agents could thus be of interest.

Glycerol, a by-product in bio-diesel production, may be available as a cheap capping agent in the hydrothermal depolymerisation of kraft lignin. Previous work utilising glycerol in the hydrothermal processing of biomass include the liquefaction of aspen wood (Pedersen et al. 2016, 2015), rice straw (Cao et al. 2016; Kashimalla et al. 2021), algae (Han et al. 2020) and kraft lignin (Umar et al. 2022). One of the results of adding glycerol was found to be a higher yield of bio-oil, defined as extracts soluble in ethyl acetate (Cao et al. 2016; Kashimalla et al. 2021; Umar et al. 2022). Pedersen et al. (2015), on the other hand, reported a lower biocrude yield, defined as extract soluble in diethyl ether (DEE), with increasing glycerol content when aspen wood was liquefied. In terms of char or solid residue, the addition of glycerol seems to reduce their content when liquefying both aspen wood (Pedersen et al. 2015) and rice straw (Kashimalla et al. 2021). However, without Na_2CO_3, increasing levels of solid residue were reported with increasing glycerol content in the reaction mixture when liquefying rice straw (Cao et al. 2016). Overall, the experimental observations suggest that the use of Na_2CO_3 together with glycerol help reduce the char yield.

Other than the work of Umar et al. (2022), there is a scarcity of information on the use of glycerol in the hydrothermal processing of kraft lignin. Yet, Umar et al. did not report any data on solid residue or char being formed during the 30–90 min of processing, which is a long residence time for this type of process. Hence, the present work aims at elucidating the effect of glycerol as a capping agent to reduce the char yield and molecular weight of the products in the depolymerisation of kraft lignin at short residence times.

2 Materials and methods

2.1 Materials

The lignin used was softwood kraft lignin (*Pinus sylvestris* and *Picea abies*), isolated from black liquor by the LignoBoost process at the Bäckhammar Mill in Sweden, with a dry content of 76.6% ± 0.4% (measured using a Sartorius MA30; Sartorius, Göttingen, Germany). Glycerol (99.9%, VWR Chemicals, Leuven, Belgium), anhydrous sodium carbonate (≥99.9%, VWR Chemicals, Leuven, Belgium), deionised water and sodium hydroxide (99–100%, Merck, Darmstadt, Germany) were used as reaction media for the depolymerisation. LiBr (>99%, Sigma-Aldrich, Steinheim, Germany), dimethyl sulfoxide (DMSO, >99.7%, Sigma-Aldrich, Steinheim, Germany), pullulan standards (PL2090-0100, Varian, Church Stretton, UK), sodium standard (UltraScientific, North Kingstown, USA), diethyl ether (DEE, >99.0% with 1 ppm BHT as inhibitor, Sigma-Aldrich, Steinheim, Germany), nitric acid (65%, Merck Suprapur, Darmstadt, Germany), syringol (99%, Sigma-Aldrich, Steinheim, Germany), DMSO-d_6 (99.5 atom % D, 0.03 (v/v) TMS, Sigma-Aldrich, Sigma-Aldrich, Steinheim, Germany), cyclohexanol (99%, Sigma-Aldrich, Steinheim, Germany), guaiacol (Sigma-Aldrich, Steinheim, Germany), 1,2-dimethoxybenzene (99%, Sigma-Aldrich, Steinheim, Germany), 4-methylguaiacol (≥98%, Sigma-Aldrich, Steinheim, Germany), 4-ethylguaiacol (≥98%, Sigma-Aldrich, Steinheim, Germany), vanillin (99% Sigma-Aldrich, Steinheim, Germany), acetovanillone (≥98%, Sigma-Aldrich, Steinheim, Germany), homovanillic acid (Sigma-Aldrich, Steinheim, Germany) and HCl (1 M, Honeywell Fluka, Seelze, Germany) were all used as received.

2.2 Methods

Kraft lignin was depolymerised in a custom-made batch reactor (SITEC-Sieber Engineering AG, Zürich, Switzerland) with a volume of 99 ml designed for rapid heating of the reaction mixture. Further details on the reactor are reported elsewhere (Arturi et al. 2017).

The reaction mixture was divided into a pre-charge comprised of only water, NaOH and Na_2CO_3, and an injection charge comprised of water, NaOH, Na_2CO_3, glycerol and lignin. NaOH was added not only as an alkaline catalyst but also to raise the pH, so that the lignin would dissolve better and the injection charge could be pumped. The injection charge was mixed with an Ultra-Turrax (T25 Digital Ultra-Turrax, IKA®-Werke GmbH & Co. KG, Staufen, Germany) for 15 min at 15 000 rpm twice, in order to disperse the lignin thoroughly while avoiding excessive foaming.

The pre-charge was added to the reactor and, before it was sealed, N_2 was used to displace air. The reactor was then pre-heated to 310 °C, causing it to reach a pressure essentially equal to the vapour pressure of water at 310 °C, i.e. approx. 100 bar. Using a hand pump, the injection charge was then injected for 51 s ± 18 s (on average, with standard deviation) into the vapour-liquid equilibrium prevailing in the reactor. The subsequent temperature drop was mitigated by the heat released from the condensation of the vapour; the temperature and pressure profiles of all the reactions are shown in Supplementary Figures S1 and S2.

The residence time was defined as the time between the end of the injection and the start of the discharge from the reactor. This meant that the temperature and pressure still rose during the reaction, since the injected material was heated. The temperature and pressure were logged every tenth second; the average temperatures and pressures during the reaction were calculated using

$$y_{avg} = \int_{t_1}^{t_2} \frac{y(t)dt}{(t_2 - t_1)}$$

where y is either pressure or temperature. At the end of the residence time, the reaction mixture was discharged and quenched into a cold trap of 200 ml of water in a flask equipped with a condenser placed in an ice-bath. The discharge took 41 s ± 12 s on average, with standard deviation.

Although the pressure of the system rose during the reaction, it was fine-tuned to the reaction pressure of 250 bar by the injection and withdrawal of reaction mixture in portions <1 ml. As the high pressure meant that the reaction was carried out in liquid phase, very small injected and withdrawn volumes were sufficient to control the pressure.

2.2.1 Test plan: The study is based on 8 experimental runs at average temperatures of 270–291 °C and average pressures of 229–258 bar. Residence times ranged between 1 and 12 min, with replicate runs at 1 and 4 min. Furthermore, reference runs at 4 min without glycerol and with NaOH, and without NaOH and with glycerol, respectively, were executed. Reaction conditions, including the composition of the reactor mixture and the pH after quenching in the cold trap, are presented in Table 1.

2.2.2 Separation: The product was separated into three fractions: char, precipitated solids (PS) and acid soluble organics (ASO), as shown in Figure 1. First, the reactor product was filtered on a #5 glass filter with a nominal cut-off of 1.0–1.6 μm. No change of the pH level of the product diluted in the cold trap water was made prior to filtering. Thus, the solid materials in the product mixture could be quantified after drying. The filter was dried for 4 days at 40 °C, after which the filter cake was denoted *char*. In most cases, the filter cake could be removed easily from the filter by scraping it off gently. However, at 1 and 2 min of residence time, the amount of char was so small that it did not form a filter cake. In these cases, the char was dissolved in DMSO, which was added to the filters, to reach a solution with a concentration 10 mg/ml char. In subsequent nuclear magnetic resonance spectroscopy (NMR) analyses, this DMSO was evaporated and the char fractions redissolved in DMSO-d_6.

The filtrate of the product was acidified with 1 M HCl to pH 1.5 (TitroLine 7000, SI Analytics; Xylem Analytics Germany GmbH, Welheim, Germany) causing precipitation and the evolution of gas as carbonates from residual Na_2CO_3 formed CO_2. The acidified mixture was filtered on glass filters #5, with a nominal cut-off of 1.0–1.6 μm. The filtrate was stored for later extraction with DEE for gas chromatography mass spectrometry (GC-MS) analysis. The filter cake was then washed with an equal amount of water as the sample volume, after which it was dried at 40 °C for 5 days, thus forming the precipitated solids (PS) fraction.

The acid filtrate was evaporated for 3 days at ambient temperature and 1 day at 40 °C. This fraction, a viscous yellow-orange liquid, was comprised of the acid soluble organics (ASO) in combination with both the residual glycerol and the NaCl from the neutralisation of Na_2CO_3 and NaOH during the acidification step. The amount of NaCl in the ASO fraction was estimated by quantifying the amount of Na in the acid filtrate by inductively-coupled plasma – optical emission spectrometry (ICP-OES). The NaCl was then deducted from the ASO. The glycerol in the ASO was quantified by gas chromatography with a thermal conductivity detector (GC-TCD), using a linear external calibration curve of glycerol standards (R^2 = 0.9957) as well as an internal standard of cyclohexanol.
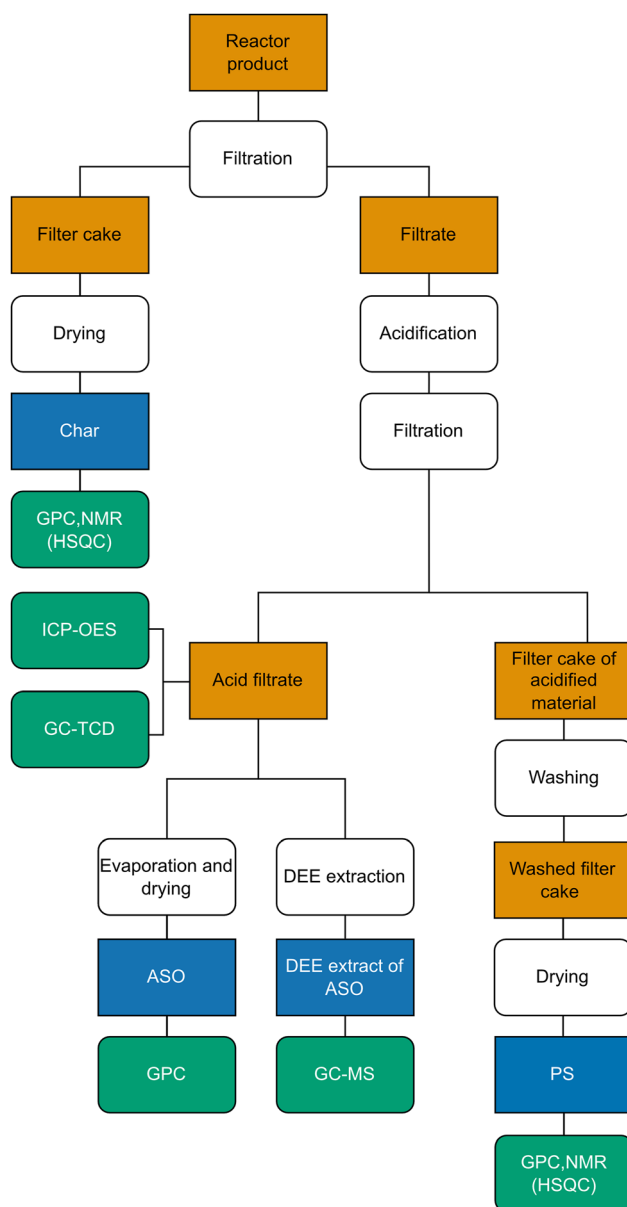

Figure 1: Flow chart of the fractionation of the reactor product.

Table 1: Average reaction temperatures and pressures in the reactor, compositions of the reaction mixture and yields of char.

Residence time (min)	T_{avg} (°C)	P_{avg} (bar)	Reaction product pH	Na_2CO_3 (wt%)	NaOH (wt%)	Water (wt%)	Glycerol (wt%)	Dry lignin (wt%)	Char yield (% dry basis)
1	281	227	10.7	1.6	1.0	75.7	15.9	5.8	3.5
1	270	229	10.5	1.6	1.0	74.7	16.5	6.1	1.5
2	272	251	10.7	1.6	1.0	75.0	16.3	6.0	1.7
4	285	249	10.4	1.6	1.0	75.9	15.7	5.8	14.4
4	281	250	10.4	1.6	1.0	76.7	15.1	5.6	12.5
12[a]	291	258	9.9	1.6	1.0	74.0–76.3	15.5–17.2	5.7-6.3	22.6–27.6
4	281	251	9.3	1.6	0.0	76.6	15.9	5.9	32.0
4[b]	290	247	10.7	1.6	1.0	92.3	0.0	5.1	4.2–4.6

[a]The amount of injection charge in the experiment at 12 min was uncertain; ranges of the glycerol, lignin and water injected are therefore given. [b]The yield of char in the sample without glycerol is somewhat uncertain and a range is therefore presented.

After quantifying the NaCl and glycerol in the yellow-orange liquid that contained the ASO, it was found that the mass fraction of ASO was small, on average 3%, whereas the NaCl amounted to 15% with the remainder being glycerol. The glycerol measurement influenced the estimation of the ASO yield significantly, since glycerol was the largest fraction in the yellow-orange liquid.

2.2.3 Analytical procedures:
The analytical procedures included gel permeation chromatography (GPC), nuclear magnetic resonance spectroscopy (NMR), inductively-coupled plasma optical emission spectroscopy (ICP-OES), gas chromatography with mass spectrometry as well as with thermal conductivity detection (GC-MS and GC-TCD).

2.2.3.1 GPC: Molecular weights of the product fractions were measured with gel permeation chromatography (GPC, PL-GPC 50 Plus Integrated GPC system, Polymer Laboratories; Varian Inc., Church Stretton, UK). Two columns (PolarGel-M, 300 × 7.5 mm) with a pre-column (PolarGel-M, 50 × 7.5 mm) were used in a system with an ultraviolet light (UV) detector operating at 280 nm. The eluent was DMSO with 10 mM LiBr and, in the case of PS and char, the samples were dissolved to a concentration of 0.24 mg/ml. The ASO samples were dissolved to 1.5 mg/ml to ensure a sufficiently strong signal because these samples also contained glycerol and NaCl. The samples were filtered with 0.2 μm GHP syringe filters and then run, in duplicate, at 50 °C with an eluent flow rate of 0.5 ml/min. The system was calibrated using pullulan standards. Data analysis was performed with Cirrus GPC Software 3.2.

2.2.3.2 NMR: Char and PS samples were investigated by recording heteronuclear single quantum coherence (HSQC) spectra on an 800 MHz spectrometer, with a 5 mm TXO cold probe (Bruker Avance III HD; Bruker BioSpin GmBH, Rheinstetten, Germany) at 25 °C. The samples were dissolved to a concentration of 140 mg/ml in DMSO-d_6 and then centrifuged at a relative centrifugal force (RCF) of 12,045 × g for 5 min to separate possible insoluble material. The supernatant was transferred to 3 mm tubes. In the case of char samples from runs with residence times of 2 and 4 min, as well as char samples from the runs without glycerol and NaOH, a little material (approx. <5%) was undissolved and was therefore not included in the analyses. The samples of PS and lignin did not show any undissolved material.

The samples were run at 25 °C using the HSQC pulse programme *hsqcedetgpsisp2.3* with acquisition times of 96 ms for ^{1}H and 6 ms for ^{13}C. A total of 3072 and 512 points were acquired for ^{1}H and ^{13}C, respectively, with 24 scans and 1 s relaxation delay. The spectra were recorded in an edited mode.

Although samples at all residence times were investigated, only one sample was used for each of the replicates at 1 and 4 min. In this case, the samples with the highest average reaction temperature were selected, see Table 1.

2.2.3.3 ICP-OES: The sodium content of the acidified filtrate was determined using ICP-OES (Thermo Scientific iCAP Pro, Thermo Fischer, Cambridge, UK). After being diluted 1:50 with 0.5 M HNO_3, triplicates were measured on the emission wavelength of 589.59 nm, with an average relative standard deviation (RSD) of 9%.

2.2.3.4 GC-TCD: The amount of glycerol present in the acid filtrate was quantified using GC (Agilent 7890A; Agilent Technologies Co. Ltd., Shanghai, China) with a TCD (G3437A; Agilent Technologies Co. Ltd., Shanghai, China).

The acid filtrate, shown in Figure 1, was diluted 1:10 with water, and an internal standard solution of cyclohexanol was added to the samples to reach a concentration of 2.05 g cyclohexanol/l. The samples were then filtered in a 0.45 μm GHP filter. A calibration curve of glycerol in water was constructed with the same concentration of internal standard as in the samples.

The injection volume was 1 μl, with a 40:1 split ratio and an inlet temperature of 300 °C. The column used was an HP-5MS UI (Agilent Technologies Inc., Santa Clara, CA, USA) and the temperature programme started at 90 °C. This was followed by heating at 15 °C/min up to 200 °C and then 60 °C/min to 310 °C, where the temperature was held for 2 min with a helium carrier gas flow of 2.1 ml/min. The TCD detector was operated at 320 °C, with a reference flow of 10 ml/min and a make-up flow of 4.5 ml/min. Samples were run in duplicate with an average RSD of 2.1%.

2.2.3.5 GC-MS: Identification of the monomeric aromatic components produced during the reaction was carried out using GC-MS (Agilent 7890A; Agilent Technologies Co. Ltd., Shanghai, China and Agilent 5975C; Agilent Technologies Inc., Wilmington, DE, USA). 0.5 ml of internal standard solution, 0.001 g/ml syringol in water, was added to 5 ml of acid filtrate. The mixture was extracted with diethyl ether (DEE) in a separating funnel at 1:1 w/w. The ether phase was then filtered through a 0.2 μm polytetrafluorethylene (PTFE) filter.

The injection volume was 1 μl, with a 19:1 split ratio and inlet temperature of 300 °C. The flow rate of the carrier gas, helium, was 1 ml/min and the column was an HP-5MS UI (Agilent Technologies Inc., Santa Clara, CA, USA). After maintaining a constant temperature of 70 °C for 2 min, it was increased by 20 °C/min to 275 °C, where it was held for 10 min. The MS source was run at 230 °C and the MS Quad at 150 °C. The compounds were identified by NIST MS Search Software (V. 2.2) utilising the library NIST/EPA/NIH Mass Spectral Library (NIST 11). Also, retention time analysis with pure compounds was performed to verify the results obtained from the NIST MS search. A semi-quantification of the products was used employing the relationship:

$$W_i = W_{IST}A_i/A_{IST},$$

where A is the peak area in the chromatogram, W the mass fraction in the sample, i the analyte in the samples and IST the internal standard (Nguyen et al. 2014). The samples were run in duplicate, with an average RSD of 5.7%.

3 Results and discussion

The product discharged from the reactor was a mixture of solid particles in an aqueous phase, with a smoky odour. The pH of the reaction mixture was decreased at longer residence times, indicating that the reactions formed products consuming OH⁻, see Table 1. Miller et al. (2002) argued that such neutralisation is caused not only by phenolic products formed during depolymerisation, but also by the CO_2 formed during the process. Moreover, the formation of acids could occur during lignin depolymerisation, which would reduce the pH (Rößiger et al. 2018).

Table 2: The weight average molecular weight (M_w) of the product fractions, with standard deviations, at 4 min of residence time with and without NaOH and glycerol, respectively.

	Char (kDa)	PS (kDa)	ASO (kDa)
LignoBoost		13.2 ± 0.3	
4 min	8.8 ± 0.1	7.5 ± 0.3	0.8 ± 0.0
4 min w/o glycerol	10.1 ± 0.1	8.7 ± 0.0	1.2 ± 0.0
4 min w/o NaOH	8.6 ± 0.0	9.6 ± 0.0	0.9 ± 0.0

The 4 min data are averages of the two experiments run with NaOH and glycerol at 4 min residence time.

3.1 Molecular weight

The weight average molecular weight (M_w) of the LignoBoost lignin feed and the product fractions, with and without NaOH and glycerol as well as at different residence times are presented with their respective standard deviations in Table 2 and Table 3. The molecular weight distributions from which these M_w are calculated are shown in Figure 2 and in Supplementary Figure S3. Samples *1 min* and *4 min* are the average values of the experiments run at these residence times.

3.1.1 Effect of glycerol and NaOH on M_w

Table 2 shows that, in all cases, the addition of glycerol reduces the M_w of the products. This could be interpreted as a capping effect, whereby glycerol reacts with reactive fragments and thus prevents repolymerisation.

Without NaOH, the M_w of the PS is higher but that of the char fraction is slightly lower, when compared to the case with NaOH (sample *4 min*). The higher pH of the reaction mixture with NaOH (sample *4 min*) thus seems to favour reactions that depolymerise the compounds in the PS fraction. The char fraction is, however, influenced to a lesser degree by the pH.

3.1.2 Effect of residence time on M_w

When the residence time is increased, the M_w decreases for both the char and PS fractions when both NaOH and glycerol

Table 3: Weight average molecular weight (M_w) of the product fractions, with standard deviations at different residence times.

	Char (kDa)	PS (kDa)	ASO (kDa)
LignoBoost		13.2 ± 0.3	
1 min	11.5 ± 0.6	8.5 ± 0.7	0.9 ± 0.0
2 min	11.6 ± 0.0	7.6 ± 0.0	0.9 ± 0.0
4 min	8.8 ± 0.1	7.5 ± 0.3	0.8 ± 0.0
12 min	6.8 ± 0.2	5.9 ± 0.0	0.9 ± 0.0

are present in the reaction system, as reported in Table 3: the samples 1 min and 4 min are averages of the duplicate reactor runs at these residence times, which explains the larger standard deviation. Thus, over the course of the residence times investigated, there is a net depolymerisation of the lignin.

The molecular weight distributions obtained from the GPC measurements are presented in Figure 2. It shows that a narrowing of the molecular weight distribution occurs after just 1 min of residence time, and that the larger molecular weight fractions gradually disappear with increasing residence times, see A and B in Figure 2.

In the case of the PS fraction, the molecular weight distributions are similar for the samples at 1, 2 and 4 min of residence time. However, there is a shift in the reaction products between 4 and 12 min, causing the distribution to shift to lower molecular weights and, consequently, causing the M_w to drop, see Table 3. It is possible that the longer residence time allows reactions with a slower kinetics time to progress, thereby giving a larger fraction of low molecular weight components. Thus, swift initial reactions that narrow the molecular weight distribution after just 1 min of residence time are followed by slower reactions.

The M_w of the ASO does not show any clear trend with increasing residence time. It can nevertheless be noted that the same peaks occur in the chromatograms of all samples, see Figure 2C, but at varying intensity: this suggests that products of similar molecular weight are formed at all of the residence times investigated but at different concentrations.

3.2 Changes in molecular structure

The char and PS fractions at all residence times were investigated with NMR using an edited HSQC pulse sequence. Neither the char nor the PS fractions showed much change at longer residence times and therefore only the results for the 1 min sample are discussed; the spectra of the other residence times are shown in Supplementary Figure S4. Figure 3 shows the inter-unit aliphatic region of the HSQC spectra for unreacted lignin, char and PS after 1 min of residence time. The peaks from the main inter-unit linkages in lignin, such as β-O-4′, β-5′, β-β′, appear due to their connections with oxygen which give chemical shifts in the regions highlighted with black rectangles.

The signals of the inter-unit ether linkages that are evident in the lignin spectrum (Figure 3A) are not found in the char and PS fractions. The structure of the original lignin thus changes during the reaction, and it does so rapidly: within 1 min of residence time. There is a trace of β-β′ signals in the PS fraction at δ_C/δ_H 85.5/4.65 ppm. This peak corresponds to the
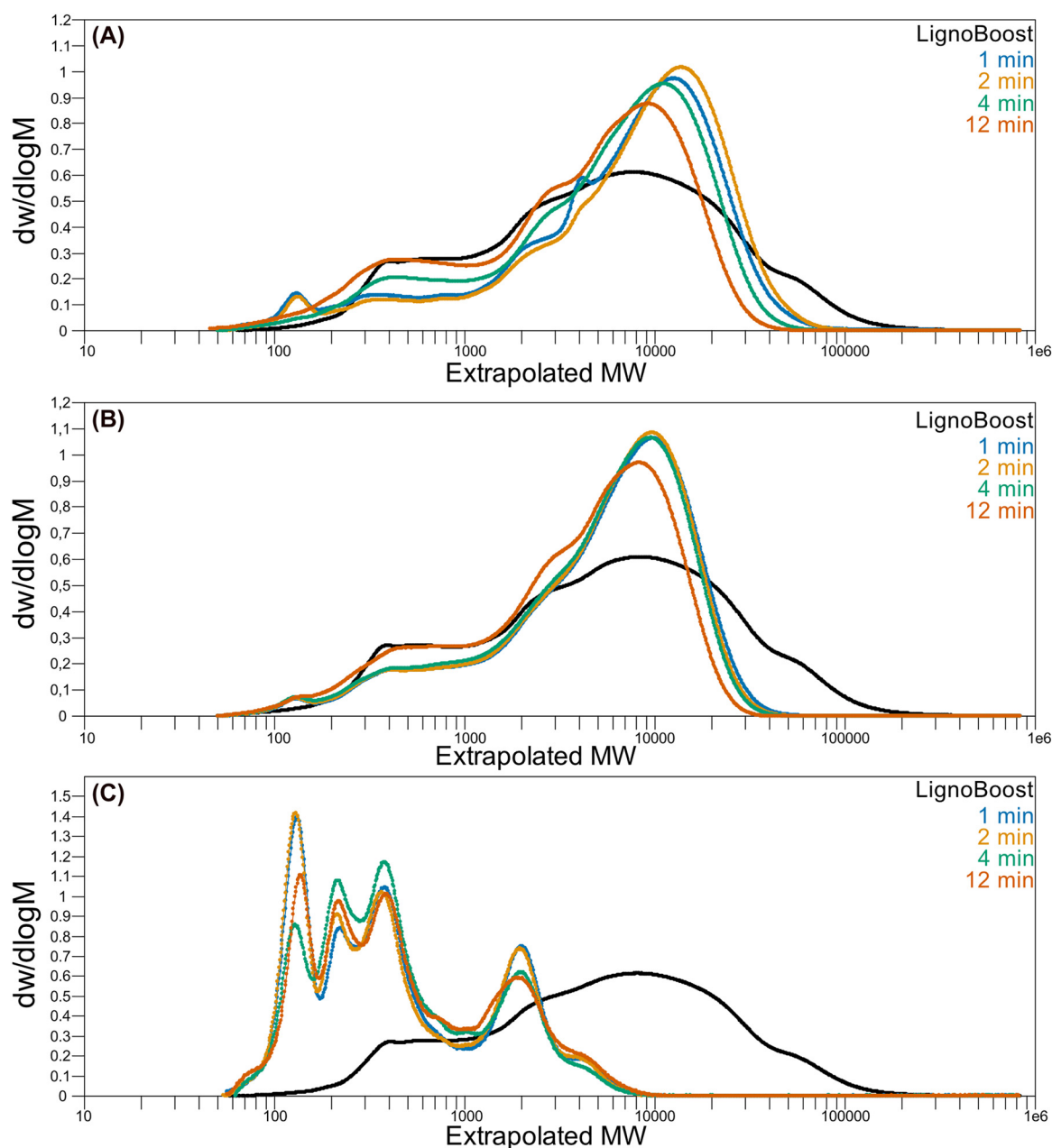
Figure 2: Molecular weight distributions of the char (A), PS (B) and ASO (C) at different residence times.

CH signal at the α position in the ether part of the β-β′ bond. It thus seems that the reaction that breaks the ether fraction of the β-β′ bond has a slower kinetics compared to the other inter-unit ether linkages, since this residual peak lingers on. However, it disappears at longer residence times, as shown in Supplementary Figure S4. Thus, over the course of the residence times investigated, there is a depolymerisation of the lignin, which agrees with the net depolymerisation seen in Table 3. While there could be a formation of new bonds, the net result of the hydrothermal treatment at these conditions is depolymerisation.

The spectra in Figure 3 show that glycerol remained in both the char and PS fractions. The latter was somewhat surprising since, unlike the char, the PS filter cake was washed with water prior to drying. Yet, some glycerol remained, showing peaks around δ_C/δ_H 63.1/(3.38 and 3.31) ppm and 72.4/3.45 ppm (National Institute of Advanced Industrial Science and Technology; AIST 1999). However, these glycerol peaks do not overlap with the peaks of interest, i.e. the lignin inter-unit ether linkages.

It is notable that there are some new peaks around δ_C/δ_H 76/4.2–4.8 ppm that are present in both the char and PS,
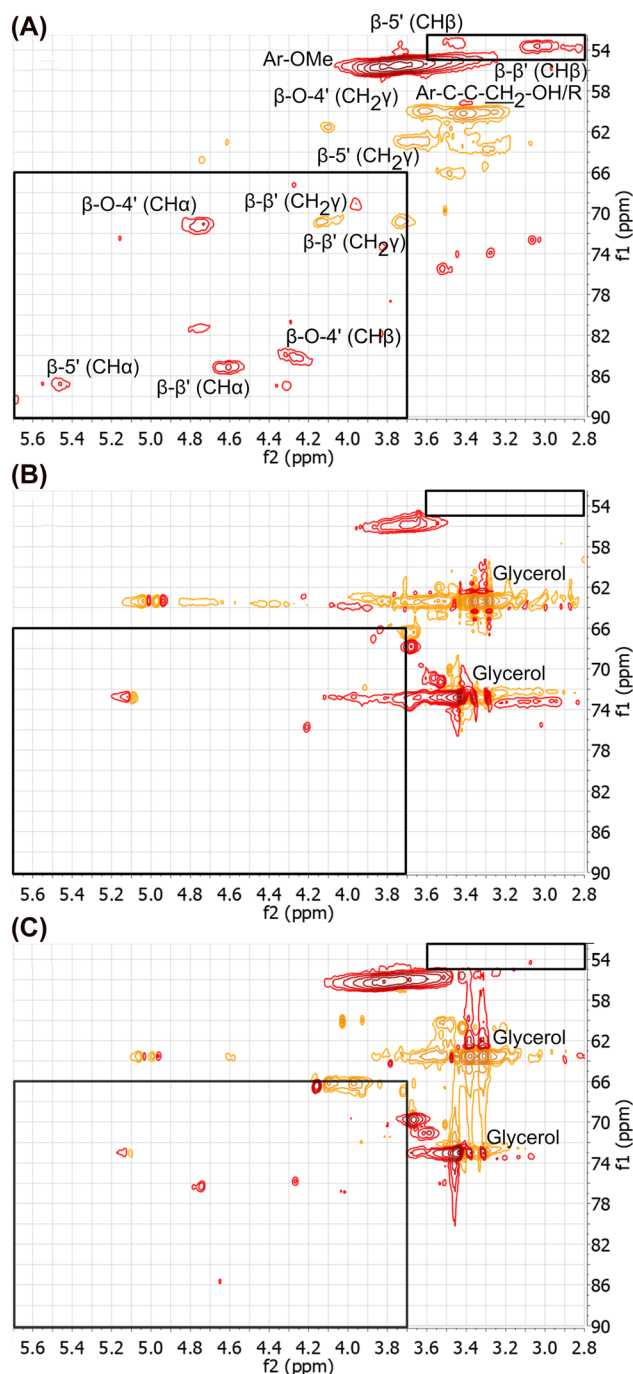
(A)

(B)

(C)

Figure 3: Inter-unit aliphatic region of the HSQC spectra of the LignoBoost lignin (A), char after 1 min of residence time (B) and PS after 1 min of residence time (C). Labelling in (A) is according to Mattsson et al. (2016) and Giummarella et al. (2020). The peaks at δ_C 63.1 and 72.4 ppm in the char (B) and PS (C) spectra are artifact peaks from the added glycerol (National Institute of Advanced Industrial Science and Technology; AIST 1999).

Figure 3B and C. These are not seen in the sample without glycerol: it may be that glycerol has some sort of bond to lignin-derived components, giving these peaks. Peaks unique to the cases with added glycerol are also seen in the aliphatic region of the HSQC spectra (not shown here), suggesting that glycerol reacts with the components and produces new structures.

Comparing the signals of char after 1 and 12 min with the starting lignin, the signals in the aromatic section of the 1 min char HSQC spectra are fairly weak, see Supplementary Figure S5. This could indicate that only a fraction of the char sample at 1 min was, in fact, examined by NMR: since very little char was produced at this residence time, it is possible that its concentration was somewhat too low. A rapid narrowing of the molecular weight distribution was nevertheless seen in the M_w measurements, see Figure 2: this agrees with our previous study at similar reaction conditions (except that isopropanol was used instead of glycerol), where significant structural changes were noted after just 1 min of residence time (Ahlbom et al. 2022). The result in the inter-unit ether linkage region after 1 min of residence time is therefore the same as in our previous work, although the aromatic region differs; the reactions appear to be rapid in this set-up, too.

3.3 Yields

The percentage yields of the dried products (i.e. char, PS and ASO) were defined with respect to the dry lignin charged to the reactor according to the following equation:

$$Y_i = 100 \cdot \frac{m_i}{m_{dry\ lignin}}$$

where m_i and Y_i are the mass and yield, respectively, of the product fraction i and $m_{dry\ lignin}$ is the mass of dry lignin loaded to the reactor.

While the char and PS contained glycerol, as seen in the NMR spectra reported in Figure 3, there was no practical way of quantifying the amount of glycerol accurately. In the ASO fraction, on the other hand, quantification was possible using GC-TCD. Thus, the yields of char and PS, presented in Figures 4 and 5, are overestimated due to the content of glycerol. The PS fraction was washed to remove most of the residual glycerol so the overestimation due to glycerol is, in fact, minor for this fraction. However, the content of glycerol in the char fraction was estimated as being as high as 24%,
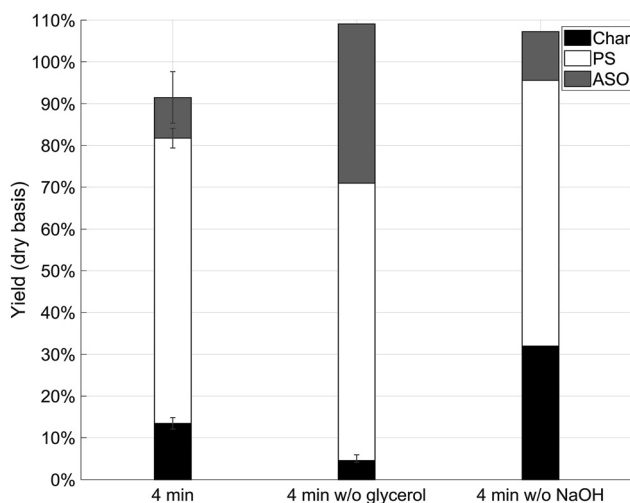
Figure 4: Yields of the fractions obtained on a dry lignin basis at 4 min residence time with and without glycerol or NaOH, respectively. The 4 min samples are the average yields from the two reactor runs at 4 min with NaOH and glycerol added, including standard deviations as the error bars. The yield of char in the sample without glycerol is somewhat uncertain and a range is therefore presented.

Figure 5: Yields of product fractions on a dry lignin basis versus residence time. Error bars give the standard deviation of the two reactor runs at 1 and 4 min, and the uncertainty in the 12 min case where the amount of lignin injected was not determined precisely.

thus leading to a large overestimation. This figure was based on the moisture content of the filter cakes before drying, combined with the glycerol content in the product phase. Nonetheless, subtracting this amount of glycerol from the char yields does not modify the trends observed.

3.3.1 Effects of NaOH and the addition of glycerol on yields

The yields of char, PS and ASO at 4 min residence time with glycerol and NaOH, and without glycerol and NaOH, respectively, are presented in Figure 4. The yield of char in the sample without glycerol is somewhat uncertain and a range is therefore presented. The dominating product fraction in all samples is the PS.

Without any NaOH in the reaction mixture but with glycerol (*4 min w/o NaOH*), the yield of char is much higher (32%, on a dry lignin basis) compared to the 13.4% ± 1.4% yield with NaOH. At these conditions, NaOH thus seems to mitigate the formation of char. It might also be that the higher pH with NaOH (10.4 vs. 9.3 without NaOH, see Table 1) causes less material to precipitate as char. The yield of PS does not change as much as the char when NaOH is added. Furthermore, without glycerol in the reaction mixture, the amount of char seems to be reduced and it seems, all in all, that glycerol is not effective in preventing char from forming at this residence time. Nevertheless, the results of the NMR measurements show that there is glycerol present in the char, see Figure 3, and this could not be quantified reliably, only estimated. If the
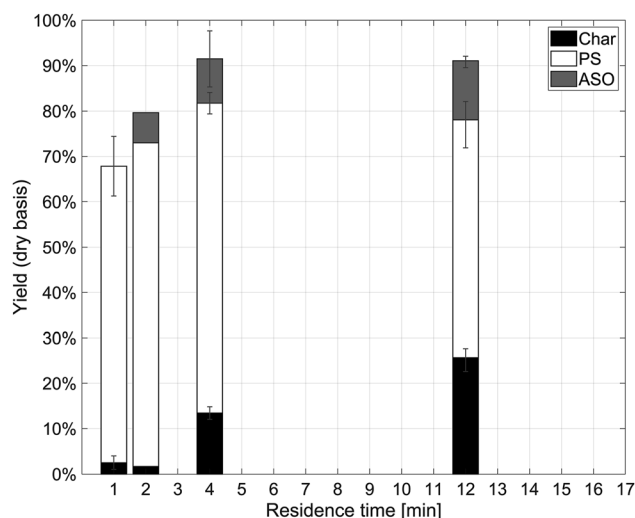
estimated 24% glycerol in the char is deducted, the sample without glycerol still has a lower char yield than the sample with glycerol added. Previous studies on aspen wood and rice straw indicate that adding glycerol could indeed reduce the amount of char formed (Kashimalla et al. 2021; Pedersen et al. 2015). Although the results obtained in this work on lignin (i.e. without the carbohydrates of aspen and rice straw) do not support a char reducing effect, they still indicate that glycerol has a capping effect that leads to the products lower having a M_w. The samples without glycerol and NaOH in Figure 4 stand out with a high overall yield, exceeding 100% of the added dry lignin suggesting an overestimation of the yield of some of the components in these samples. However, the closure of the mass balances was typically within ±10%, at most ±32%, in line with typical values reported in the literature for batch reactor studies on lignin and biomass (Lee et al. 2016; Ye et al. 2012).

3.3.2 Effect of residence time on yields

The yields of the product fractions at varying residence times are given in Figure 5 with standard deviations for the replicates at 1 and 4 min of residence time. At 12 min, the amount of injected lignin was somewhat uncertain, and the error bars show the span of values covering this uncertainty.

The yield of the dominating PS fraction decreases with residence time while the char yield increases. Although the yield of char is small at the beginning of the reaction, more is produced when the residence time is increased to 4 min, and even more at 12 min even though the M_w is reduced, see Table 3. The ASO yield also seems to increase at longer

residence times. With the char yield increasing with increasing residence time, and the PS decreasing, it thus appears that some parts of the reaction mixture that form the PS fraction at shorter residence times, react further to form char and ASO at longer residence times.

For the shortest residence time (1 min), the amount of ASO produced was too small to be quantified with accuracy. It is, however, worth mentioning that it was possible to isolate some ASO from the 1 min run, which was used to determine the molecular weight distribution, see Figure 2C, and was found to be similar to the samples run at longer residence times. This proves that some ASO is produced even at 1 min. The yields of ASO for the remainder of the samples concur with previous work (Ahlbom et al. 2022).

3.4 Monoaromatic compounds

All of the compounds identified by GC-MS in the ether extract of the acid filtrate were aromatic. The quantification is semi-quantitative, with the main component in the product being identified as guaiacol (2-methoxyphenol). This is a common product when softwood kraft lignin is depolymerised because softwood lignin monomers contain the guaiacyl group. The quantities of the monoaromatic products can be seen in Figures 6 and 7, with their respective standard deviations as error bars.

3.4.1 Effects of glycerol and NaOH on the yield of monoaromatic products

Figure 6 shows the yields of monoaromatic compounds in the cases without glycerol and NaOH and, as can be seen, no remarkable effect of glycerol is observed on the yields of the monoaromatic compounds. The effect of an NaOH addition, on the other hand, is evident: the yield of all types of compounds is higher when there is NaOH in the system. The reference sample, *4 min* in Figure 6, is the average yields of the two reactor runs at 4 min that had product pH values 10.4. However, the sample without NaOH had a pH of 9.3, see
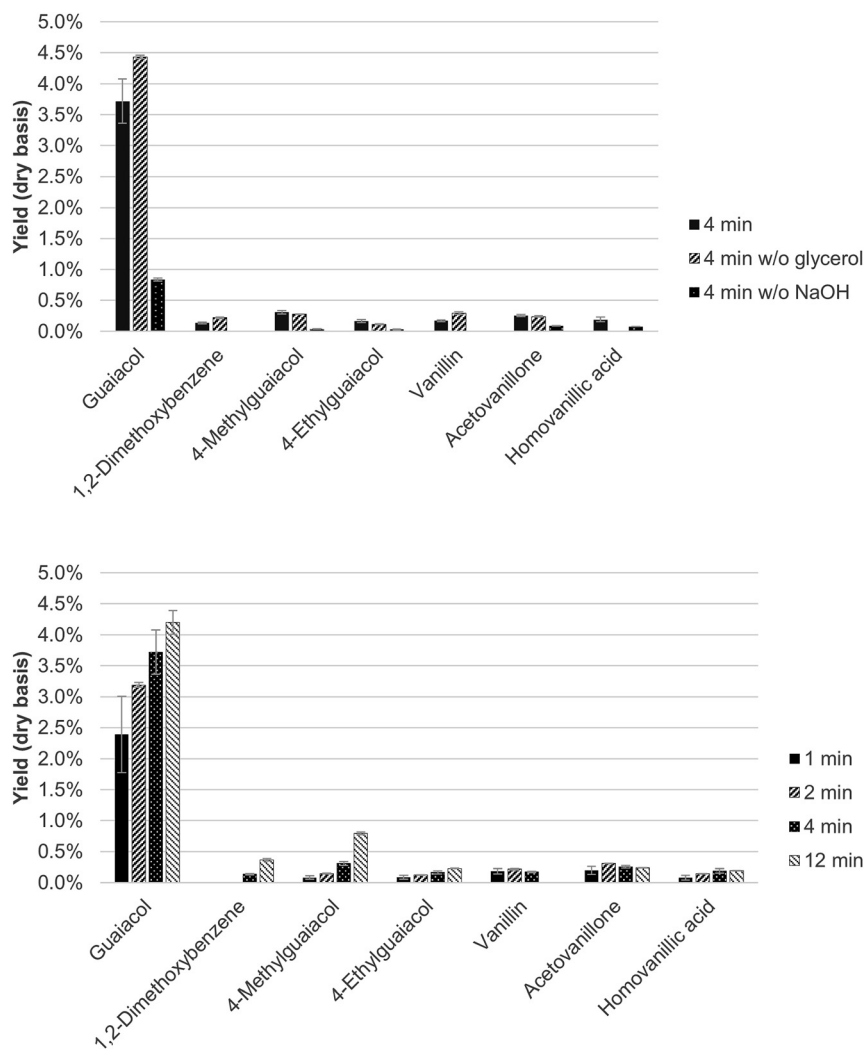

Figure 6: Compounds identified by GC-MS in the samples run at 4 min of residence time with glycerol and NaOH as well as without glycerol and NaOH, respectively, and their respective yields, with standard deviations versus dry lignin from the semi-quantitative analysis.

Figure 7: Compounds identified by GC-MS in samples run with NaOH and glycerol at different residence times, and their respective yields versus dry lignin from the semi-quantitative analysis with standard deviations.

Table 1. It seems that this pH difference influences the reactions so that the higher pH samples attain a higher yield of monoaromatic components.

3.4.2 Effect of residence time on the yield of monoaromatic products

As with the molecular weight distributions of the ASO fraction, see Figure 2C, where the same peaks were seen for all residence times, the same monoaromatic compounds are identified for all residence times. The yield of guaiacol increases with residence time, along with 1,2-dimethoxybenzene, 4-methylguaiacol and 4-ethylguaiacol, see Figure 7. Compared to our study in which isopropanol was used as a capping agent instead of glycerol (Ahlbom et al. 2022), the yields of all components are higher. This could possibly be an effect of the higher pH in the reactions of this study due to the addition of NaOH.

4 Conclusions

The dominating product fraction of the three fractions obtained when depolymerising softwood kraft lignin in water with glycerol is the precipitated solids (PS). The yield of this fraction decreases with residence time whereas the yield of the char fraction increases. The formation of char can therefore be minimised by keeping the residence time short.

Although adding glycerol to mitigate repolymerisation was effective in the sense that the M_w of all of the product fractions were reduced, it nevertheless did not reduce the yield of char.

The addition of NaOH to the reaction mixture appears to be beneficial because the char yield was reduced. Also, more monoaromatic components were produced.

As early as within the first minute of reaction, the M_w distributions show a clear reduction in large molecular weight compounds, which is also supported by NMR spectra showing that the inter-unit ether linkages break. Increasing the residence time further causes a net depolymerisation of the product fractions. In line with this, the yield of monoaromatic components also increases with residence time. Kraft lignin thus can be depolymerised in a rapid manner within the residence times investigated (1–12 min).

References

Ahlbom, A., Maschietti, M., Nielsen, R., Lyckeskog, H., Hasani, M., and Theliander, H. (2021). Using oisopropanol as a capping agent in the hydrothermal liquefaction of kraft lignin in near-critical water. Energies 14: 932.

Ahlbom, A., Maschietti, M., Nielsen, R., Hasani, M., and Theliander, H. (2022). Towards understanding kraft lignin depolymerisation under hydrothermal conditions. Holzforschung 76: 37–48.

Arturi, K.R., Strandgaard, M., Nielsen, R.P., Søgaard, E.G., and Maschietti, M. (2017). Hydrothermal liquefaction of lignin in near-critical water in a new batch reactor: influence of phenol and temperature. J. Supercrit. Fluids 123: 28–39.

Belkheiri, T., Vamling, L., Nguyen, T.D.H., Maschietti, M., Olausson, L., Andersson, S.-I., Åmand, L.-E., and Theliander, H. (2014). Kraft lignin depolymerization in near-critical water: effect of changing co-solvent. Cellul. Chem. Technol. 48: 813–818.

Belkheiri, T., Andersson, S.-I., Mattsson, C., Olausson, L., Theliander, H., and Vamling, L. (2018). Hydrothermal liquefaction of kraft lignin in subcritical water: influence of phenol as capping agent. Energy Fuel. 32: 5923–5932.

Cao, L., Zhang, C., Hao, S., Luo, G., Zhang, S., and Chen, J. (2016). Effect of glycerol as co-solvent on yields of bio-oil from rice straw through hydrothermal liquefaction. Bioresour. Technol. 220: 471–478.

Carr, A.G., Mammucari, R., and Foster, N.R. (2011). A review of subcritical water as a solvent and its utilisation for the processing of hydrophobic organic compounds. Chem. Eng. J. 172: 1–17.

Castello, D., Pedersen, T.H., and Rosendahl, L.A. (2018). Continuous hydrothermal liquefaction of biomass: a critical review. Energies 11: 3165.

Cheng, S., Wilks, C., Yuan, Z., Leitch, M., and Xu, C. (2012). Hydrothermal degradation of alkali lignin to bio-phenolic compounds in sub/supercritical ethanol and water-ethanol co-solvent. Polym. Degrad. Stabil. 97: 839–848.

Cheng, Y., Zhou, Z., Alma, M.H., Sun, D., Zhang, W., and Jiang, J. (2016). Direct liquefaction of alkali lignin in methanol and water mixture for the production of oligomeric phenols and aromatic ethers. J. Biobased Mater. Bioenergy 10: 76–80.

Dunn, K.G. and Hobson, P.A. (2016). Hydrothermal liquefaction of lignin. In: O'Hara, I. and Mundree, S. (Eds.), *Sugarcane-based biofuels and bioproducts*. John Wiley & Sons, Hoboken, New Jersey, pp. 165–206.

Giummarella, N., Lindén, P.A., Areskogh, D., and Lawoko, M. (2020). Fractional profiling of kraft Lignin structure: unravelling insights on lignin reaction mechanisms. ACS Sustain. Chem. Eng. 8: 1112–1120.

Han, Y., Hoekman, K., Jena, U., and Das, P. (2020). Use of co-solvents in hydrothermal liquefaction (HTL) of microalgae. Energies 13: 124.

Kashimalla, M., Suraboyina, S., Dubbaka, V., and Polumati, A. (2021). Optimisation of a catalytic hydrothermal liquefaction process using

central composite design for yield improvement of bio-oil. Biomass Convers. Biorefinery, https://doi.org/10.1007/s13399-021-01451-8.

Kruse, A. and Dahmen, N. (2015). Water – a magic solvent for biomass conversion. J. Supercrit. Fluids 96: 36–45.

Lappalainen, J., Baudouin, D., Hornung, U., Schuler, J., Melin, K., Bjelić, S., Vogel, F., Konttinen, J., and Joronen, T. (2020). Sub- and supercritical water liquefaction of kraft lignin and black liquor derived lignin. Energies 13: 3309.

Lee, H.-S., Jae, J., Ha, J.-M., and Suh, D.J. (2016). Hydro- and solvothermolysis of kraft lignin for maximizing production of monomeric aromatic chemicals. Bioresour. Technol. 203: 142–149.

Mattsson, C., Andersson, S.I., Belkheiri, T., Åmand, L.E., Olausson, L., Vamling, L., and Theliander, H. (2016). Using 2D NMR to characterize the structure of the low and high molecular weight fractions of bio-oil obtained from LignoBoost^{TM} kraft lignin depolymerized in subcritical water. Biomass Bioenergy 95: 364–377.

Miller, J.E., Evans, L., Mudd, J.E., and Brown, K.A. (2002). Batch microreactor studies of lignin depolymerization by bases. 2. Aqueous solvents. Sandia National Laboratories Report, SAND2002-1318.

National Institute of Advanced Industrial Science and Technology; AIST (1999). Glycerol. Spectr. Database Org. Compd. SDBS, Available at: https://sdbs.db.aist.go.jp/sdbs/cgi-bin/landingpage?sdbsno=2517 (Accessed 6 December 2022).

Nguyen, T.D.H., Maschietti, M., Belkheiri, T., Åmand, L.E., Theliander, H., Vamling, L., Olausson, L., and Andersson, S.I. (2014). Catalytic depolymerisation and conversion of kraft lignin into liquid products using near-critical water. J. Supercrit. Fluids 86: 67–75.

Otromke, M., White, R.J., and Sauer, J. (2019). Hydrothermal base catalyzed depolymerization and conversion of technical lignin – an introductory review. Carbon Resour. Convers. 2: 59–71.

Pedersen, T.H., Jasiunas, L., Casamassima, L., Singh, S., Jensen, T., and Rosendahl, L.A. (2015). Synergetic hydrothermal co-liquefaction of crude glycerol and aspen wood. Energy Convers. Manag. 106: 886–891.

Pedersen, T.H., Grigoras, I.F., Hoffmann, J., Toor, S.S., Daraban, I.M., Jensen, C.U., Iversen, S.B., Madsen, R.B., Glasius, M., Arturi, K.R., et al. (2016). Continuous hydrothermal co-liquefaction of aspen wood and glycerol with water phase recirculation. Appl. Energy 162: 1034–1041.

Peterson, A.A., Vogel, F., Lachance, R.P., Fröling, M., Antal, M.J., and Tester, J.W. (2008). Thermochemical biofuel production in hydrothermal media: a review of sub- and supercritical water technologies. Energy Environ. Sci. 1: 32–65.

Roberts, V.M., Stein, V., Reiner, T., Lemonidou, A., Li, X., and Lercher, J.A. (2011). Towards quantitative catalytic lignin depolymerization. Chem. Eur J. 17: 5939–5948.

Rößiger, B., Unkelbach, G., and Pufky-Heinrich, D. (2018). Base-catalyzed depolymerization of lignin: history, challenges and perspectives. In: Poletto, M. (Ed.), *Lignin - trends and applications*. IntechOpen, London, UK, London, pp. 99–120.

Saisu, M., Sato, T., Watanabe, M., Adschiri, T., and Arai, K. (2003). Conversion of lignin with supercritical water-phenol mixtures. Energy Fuel. 17: 922–928.

Umar, Y., Velasco, O., Abdelaziz, O.Y., Aboelazayem, O., Gadalla, M.A., Hulteberg, C.P., and Saha, B. (2022). A renewable lignin-derived bio-oil for boosting the oxidation stability of biodiesel. Renew. Energy 182: 867–878.

Ye, Y., Zhang, Y., Fan, J., and Chang, J. (2012). Novel method for production of phenolics by combining lignin extraction with lignin depolymerization in aqueous ethanol. Ind. Eng. Chem. Res. 51: 103–110.

Yoshikawa, T., Yagi, T., Shinohara, S., Fukunaga, T., Nakasaka, Y., Tago, T., and Masuda, T. (2013). Production of phenols from lignin via depolymerization and catalytic cracking. Fuel Process. Technol. 108: 69–75.